HHS Public Access

Author manuscript

Nat Immunol. Author manuscript; available in PMC 2017 August 13.

Published in final edited form as:

Nat Immunol. 2017 April ; 18(4): 464–473. doi:10.1038/ni.3684.

Defining the antibody cross-reactome against the influenza virus surface glycoproteins

Raffael Nachbagauer[1], **Angela Choi**[1,2], **Ariana Hirsh**[1], **Irina Margine**[1], **Sayaka Iida**[3], **Aldo Barrera**[4], **Marcela Ferres**[4], **Randy A. Albrecht**[1,5], **Adolfo García-Sastre**[1,5,6], **Nicole M. Bouvier**[1,6], **Kimihito Ito**[3], **Rafael A. Medina**[1,4,7], **Peter Palese**[1,6], and **Florian Krammer**[1]

[1]Department of Microbiology, Icahn School of Medicine at Mount Sinai, New York, New York, USA

[2]Graduate School of Biological Sciences, Icahn School of Medicine at Mount Sinai, New York, New York, USA

[3]Division of Bioinformatics, Hokkaido University Research Center for Zoonosis Control, Kitaku, Japan

[4]Departamento de Infectología e Inmunología Pediátrica, School of Medicine, Pontificia Universidad Católica de Chile, Santiago, Chile

[5]Global Health and Emerging Pathogens Institute, Icahn School of Medicine at Mount Sinai, New York, New York, USA

[6]Department of Medicine, Icahn School of Medicine at Mount Sinai, New York, New York, USA

[7]Millennium Institute on Immunology and Immunotherapy, Pontificia Universidad Católica de Chile, Santiago, Chile

Summary

Influenza virus infections induce antibodies against the viral surface glycoproteins hemagglutinin and neuraminidase, and these responses can be broadly protective. To test the breadth and magnitude of antibody responses, mice, guinea pigs and ferrets were sequentially infected with divergent H1N1 or H3N2 viruses. Antibody responses were measured by ELISA against an extensive panel of recombinant glycoproteins representing the viral diversity in nature. Guinea pigs developed high titers of broadly cross-reactive antibodies; mice and ferrets exhibited narrower humoral responses. Then, we compared antibody responses after H1N1 or H3N2 infections in humans and found markedly broad responses and cogent evidence for original antigenic sin. This

Correspondence should be addressed to F.K. (florian.krammer@mssm.edu).

Author Contributions Statement

R.N., A.C., A.H., I.M. and F.K. performed serological experiments. R.N., A.C., I.M., N.M.B., R.A.A. and F.K. performed animal experiments. A.B., M.F. and R.A.M. acquired clinical samples and performed all necessary experiments to characterize the clinical samples. R.N., S.I., A.G.S., K.I., R.A.M. and F.K. performed data analysis. R.N., R.A.A., P.P., A.G.S. and F.K. contributed to the overall concept, experimental design and hypothesis and wrote the manuscript.

Competing Financial Interests Statement

The authors have no competing interests.

Data availability

The data that support the findings of this study are available from the corresponding author upon request.

work will inform universal influenza vaccine design and can guide pandemic preparedness efforts against emerging influenza viruses.

Introduction

Seasonal influenza virus infections cause significant morbidity and mortality every year on a global scale[1,2]. In addition, influenza pandemics occur at irregular intervals and can claim millions of human lives[3]. Current seasonal vaccines are considered an efficacious countermeasure to prevent influenza virus infection[2]. However, they usually induce strain specific immune responses towards the three to four strains included in the vaccine formulation. In contrast, infection with influenza viruses can cause broader immune responses and longer lasting protection from re-infection by the same virus subtypes[4–7].

Protective humoral immune responses against influenza viruses are usually associated with antibodies against the surface glycoproteins hemagglutinin (HA) and neuraminidase (NA). These proteins are readily accessible on the virion itself or on infected cells to antibodies and antibodies that bind to them can often inhibit virus replication *in vitro*. The traditional correlate of protection for seasonal influenza virus vaccines is based on antibodies that exhibit hemagglutination inhibition (HI) activity. They block the interaction of the receptor binding domain located on the HA head with its sialic acid receptor[8]. Due to the high plasticity and ever changing nature of the HA head domain most antibodies that exhibit this function are relatively strain specific[9,10]. Antibodies against the NA can block its enzymatic function (NA inhibition, NI) and NI active antibodies interfere with virus release and possibly also block the efficient migration of the virus through mucosal fluids and contribute to protection from disease[11,12]. NA-reactive antibodies have been shown to be broadly reactive within the subtype but usually do not exhibit heterosubtypic activity[13,14]. A third species of antibodies that exerts *in vitro* neutralizing activity are HA stalk-reactive antibodies. Due to the conserved nature of the HA stalk, these antibodies are often cross-reactive within and across HA subtypes. Most stalk-reactive antibodies - with rare exceptions - are restricted in binding to group 1 (H1, H2, H5, H6, H8, H9, H11, H12, H13, H16, HA-like H17, HA-like H18) or group 2 (H3, H4, H7, H10, H14, H15) HAs[15–18].

Importantly, as a forth antibody species, cross-reactive antibodies can also confer protection *in vivo* without showing *in vitro* neutralizing activity. Several mechanisms including antibody dependent cell-mediated cytotoxicity (ADCC), antibody dependent cellular phagocytosis (ADCP) and complement dependent cytotoxicity (CDC) have been postulated to contribute to non-neutralizing cross-protection *in vivo*[19–23]. ADCC has been recently shown to play a major role in the protective efficacy of HA stalk-reactive antibodies as well[24]. These effector functions can be assayed through *in vivo* serum transfer challenge experiments, e.g. in the mouse model[25,26].

Cross-reactive antibodies are potentially important for protection from infection with drifted (seasonal) and shifted (pandemic) influenza viruses but their prevalence and functionality is not well understood. Their presence might offer some protection - including lowering morbidity and mortality - during pandemics. A better understanding of cross-reactive immunity in the human population is also important for the development of universal

influenza vaccine strategies that are designed to boost pre-existing antibodies to protective levels. Here we analyze the cross-reactome against the influenza surface glycoproteins HA and NA induced by infection in three animal models and in humans, as well as the prevalence of cross-reactive antibodies in the general human population.

Results

Cross-reactive antibody profiles in animal models

To assess induction of cross-reactive antibodies, mice, guinea pigs and ferrets were sequentially infected with two divergent H1N1 or H3N2 influenza virus strains (Supplementary Fig. 1). The virus strains were chosen with the intention to reflect a consecutive exposure history that is consistent with strains that recently circulated in humans and because these strains replicate well in mice, guinea pigs and ferrets (Supplementary Fig. 2). Furthermore, the animal species were chosen because they are the most relevant and most widely used animal models for influenza virus research. For H1N1 the pre-pandemic, 1999 seasonal strain A/New Caledonia/20/99 (NC99) was chosen as primary infection followed by the antigenically distinct 2009 pandemic H1N1 isolate A/Netherlands/602/09 (NL09 - an isolate antigenically identical to the A/California/04/09 [Cal09] prototype pandemic H1N1 strain). Primary infection of mice led to induction of antibodies that mainly targeted the HA of the homologous strain but also bound to heterologous H1 HAs and other related group 1 HAs (Fig. 1a). Re-infection with the antigenically distinct NL09 H1N1 strain considerably boosted the broad anti-H1 antibody response as well as increased reactivity to heterosubtypic group 1 HAs (Fig. 1b). Interestingly, reactivity was highest against the H1 FM47 HA (phylogenetically situated between the HAs of the two infecting strains). In general, reactivity to group 2 HAs was low or absent (H3 HAs).

For the H3N2 arm of the experiment, animals were infected with the 1982 isolate A/Philippines/2/82 (Phil82) followed by a more recent 2011 isolate A/Victoria/361/11 (Vic11) - two strains that are separated by 29 years of antigenic drift (Supplementary Fig. 1). Primary infection with Phil82 in mice induced an immune response focused on the Phil82 H3 HA with moderate cross-reactivity to other H3 HAs and low reactivity to heterosubtypic group 2 HAs (Fig. 1c). Interestingly, low reactivity was also detected against several phylogenetically distant group 1 HAs, including H2 and H6. Re-infection with the antigenically distinct Vic11 virus broadened the immune responses to heterologous H3 and heterosubtypic group 2 HAs (Fig. 1d). Also, the reactivity to specific group 1 HAs was boosted. This cross-reactivity is noteworthy since antibodies capable of binding to the head domain of both H3 and H2 HAs have previously been isolated from human donors[27].

Reactivity towards the NA after single infection with NC99 H1N1 in the mouse model was focused to the N1 subtype (Fig. 2a). Anti-N1 reactivity was boosted but no broadening of the response was detected after the second infection (NL09 H1N1) (Fig. 2b). The NA response after H3N2 infections was similarly narrow as the one detected after H1N1 infections (Fig. 2c,d).

Next, we compared the humoral cross-reactomes of mice, guinea pigs and ferrets (Supplementary Fig. 3 and 4). All three animal models are used for influenza virus vaccine

research and intrinsic differences in each model's ability to induce cross-reactive antibodies might have important implications on the interpretation of pre-clinical data generated for HA- and NA-based (universal) influenza virus vaccine candidates. While heat-map/tree combinations are informative, they do not allow for easy comparison of the cross-reactomes of different animal models. We thus plotted the reactivity (expressed as endpoint titers) on the *y*-axis against the amino acid distance of the HAs (*x*-axis) (Fig. 3 and Supplementary Fig. 5). The resulting graphs show two-dimensional reactivity profiles that allow to visually compare the magnitude and breadth of responses between animal models. While amino acid distances do not always correlate exactly with antigenic distances, we found it to be an adequate surrogate measure for the purposes of our data representation.

For sequential H1N1 infection, our analysis shows that mice mount high antibody titers against the homologous and related HAs from the same subtype but significantly lower titers against distantly related HAs (Fig. 3a). Guinea pigs exhibit a very broad plateau of cross-reactivity. Titers against the homologous H1 HA are as high as titers against other distant group 1 HAs (Fig. 3b). Finally, ferrets induced lower titers and narrow responses (Fig. 3c). Data from sequential infection with H3N2 viruses largely echoed these findings. Narrower trends were observed for the anti-NA response with low cross-group reactivity of guinea pigs after H3N2 infection (Fig. 2, Supplementary. Fig. 3 and 4).

Our data suggest that guinea pigs have the intrinsic ability to mount broader antibody responses to influenza virus HAs than mice or ferrets. Mice show an intermediate level of breadth and ferrets - the gold standard animal model for influenza virology - show low titers and little cross-reactivity. The number of N-linked glycosylation sites on the HAs used as substrate, which could influence cross-reactivity, did not seem to correlate with antibody titers (Supplementary Fig. 6).

Cross-reactive antibody profiles in infected humans

After mapping the antibody cross-reactome induced by infection in animal models against the influenza surface glycoproteins we measured the human response to infection. We tested sera from human patients who were admitted to the hospital and were diagnosed with pandemic H1N1 or seasonal H3N2 infection. The cohort included 11 males and 8 females with 5 individuals below 18 years, 6 individuals between 18 and 59 years and 8 individuals above 59 years of age (Supplementary Table 1). Serum samples were taken on the day of admission and 21 or 28 days post admission and antibody induction was tested with a panel of recombinant HA and NA proteins. Interestingly, pandemic H1N1 infected patients induced a very broad response. The induction was highest against group 1 HAs (ranging from 10-fold to 20-fold) but the boost against group 2 HAs was almost as strong (ranging from 7-fold to 9-fold) (Fig. 4a–c, Supplementary Fig. 7 and Supplementary. Fig. 8 for absolute titers). Antibodies against influenza B virus HA were not boosted, which indicates that the measured increase in reactivity was influenza A antigen specific.

H3N2 infection in humans induced a very different antibody profile. Reactivity to the homologous strain was induced (20-fold) while the induction to the next closest H3 strain was significantly lower (8-fold) indicating that the infection induced primarily strain specific antibodies (Fig. 4d,e). Induction was also observed against more distantly related group 2

HAs while reactivity to group 1 HAs only increased marginally. Again, anti-influenza B HA antibodies were not induced. When visualized as antigenic landscapes (Fig. 4c,f) these differences become very clear. In summary, these data suggest that in humans pandemic H1N1 infection induces a broader antibody response than infection with a seasonal H3N2 virus.

The HA of pandemic H1N1 differs substantially from the HA of seasonal H1N1 strains to which humans have previously been exposed while seasonal H3N2 has been circulating in humans for several decades[5,28]. Our data therefore support the hypothesis that secondary exposure to a highly divergent HA from the same HA group induces strong cross-reactive antibody responses. Interestingly, (homologous) anti-NA responses were stronger after H3N2 infection than after H1N1 infection (Supplementary. Fig. 9).

Evidence for OAS in the human cross-reactome at baseline

Assessing the immediate immune response to acute influenza virus infections is highly important. However, measuring the cross-reactive antibody titers in the general human population in the absence of any immune perturbation provides a better understanding of potential protection in the context of pandemic preparedness. In addition, the baseline titers of cross-reactive antibodies might significantly impact on the efficacy of (universal) influenza virus vaccines[29]. Here we analyzed serum samples from 90 individuals from a gender-balanced US cohort.

To gain more insight into the changes of antibody titers over time due to exposure to influenza viruses the samples were stratified into three age groups: Individuals aged 18–20 (young), 33–44 (middle-aged, born after the H2N2 virus subtype stopped circulating) and 49–64 (experienced, potential prior exposure to the H2N2 virus subtype) (Fig. 5a). Interestingly, the different exposure history of the three age groups led to measurable differences in their cross-reactomes, including the breadth of the antibody response. The antigenic landscape of the 18–20-year-old group exhibited high titers against recent H1 and H3 with low cross-reactivity to moderately distant group 1 (H5) and group 2 (H4, H14) HAs (Fig. 5b). 33–44-year-olds had significantly higher reactivity to H1 and H3 HAs. Reactivity was particularly high against HAs that are similar to H1 and H3 viruses which circulated during the childhood of these individuals (Fig. 5c) and lower to more recent H1 and H3 strains. This group also had considerable cross-reactivity to H2 and H5 (group 1) and H4 and H14 (group 2). The 49–64-year-old cohort showed medium reactivity to both H1 and H3 but had a surprisingly high reactivity to H2 HA which is the subtype to which this group might have been first exposed to during childhood (Fig. 5d). This group also exhibits high reactivity to H5 and H18, suggesting that exposure to H2 followed by H1 boosted broadly cross-reactive antibodies (heat maps of endpoint titers are shown in Supplementary Fig. 10)[30]. Anti-NA titers were in general low and mostly confined to the N1 and N2 subtype (Supplementary. Fig. 10). An exception are the high titers against N2 from the 1957 and 1968 pandemic viruses in the 49–64-year-olds (Supplementary Fig. 10f). These data provide compelling evidence that childhood exposure to an influenza virus induces long lasting immune responses that can be measured by ELISA in adults, which supports the hypothesis of original antigenic sin.

Functionality of human cross-reactive antibodies

Antibody binding to diverse HAs and NAs provides general information about the prevalence of cross-reactive antibodies in human sera. However, it is also important to study the biological activity of the detected antibody responses. Antibodies can protect via direct inhibition/neutralization of virus and/or via Fc-mediated effector functions. Direct inhibition/neutralization can be assessed in micro-neutralization assays *in vitro*.

Here we used an assay setup that enhanced sensitivity by using multicycle virus growth in combination with purified IgG to minimize unspecific inhibition. We investigated only HA-specific antibodies, which was achieved by using re-assortant viruses that express irrelevant NAs (Supplementary Fig. 10b, d, f). We created six re-assortant viruses in the A/PR/8/34 backbone for this purpose: H1N8 (H1 from NC99), H5N8 (H5 from VN04), H9N4 (H9 from gfHoKo99), H3N8 (H3 from Phil82), H4N8 (H4 from duckCzech56) and H7N8 (H7 from Shanghai13). These viruses were selected to test if the antibody titers measured by ELISA translated into a functional assay. IgG of the 90 individuals described above were purified, reconstituted to the original concentration in serum and were tested against all six viruses.

Neutralizing activity against H1N8 was high for all age groups, as expected. One hundred percent of the young, 93.3% of the middle aged and 80% of the experienced cohort reached a titer of at least 1:40 (Fig. 6a, b). Neutralizing activity in all cohorts was low against H5N8 with only one individual in the middle aged group reaching a 1:40 titer (3.3%). However, higher neutralizing activity was detected for H9N4 with 23.3% of the young and middle aged and 33.3% of the experienced cohort developing titers of at least 1:40. Similarly, neutralizing activity against H3N8 (group 2) was high with 40% of the young, 100% of the middle aged and 86.7% of the experienced individuals developing titers of 1:40 (Fig. 6c, d). Neutralizing activity against H4N8 (0%, 16.7% and 3.3%) and H7N8 (0%, 13.3% and 10%) was considerably lower than against H3N8 but still detectable.

Neutralization titers in general correlate with ELISA titers and pre-exposure history of specific age groups. All individuals were likely exposed to the NC99 H1N1 strain, but titers inversely correlated with age: H1N8 titers were slightly higher in the young and were lowest in the experienced individuals. The young individuals lacked a strong neutralizing response against H3N8 which expresses an HA (Phil82) to which they have not been previously exposed. H3 titers were highest in the middle-aged group who were likely exposed to a strain similar to Phil82 H3N2 early in life, and were slightly lower in the experienced individuals who were likely to have been first exposed to H1N1 and/or H2N2 viruses.

In vitro neutralization assays do not capture Fc-FcR mediated mechanisms of protection, which might enhance the potency of antibodies *in vivo*[24,26]. To explore the *in vivo* potency of sera from the three cohorts described above we performed serum transfer challenge experiments in the mouse model (Supplementary. Fig. 11). Upon serum transfer mice were challenged with the H3N8, H4N8 or H7N8 viruses used in the neutralization assay above. Lungs were harvested on day 3 and on day 6 post-infection and the lung virus titers were assessed by plaque assay. For H3N8 only a small reduction was seen on day 3 post-infection in mice passively immunized with serum as compared to mice that received an

immunoglobulin-depleted serum (Fig. 6e). However, a statistically significant reduction was observed for all three groups on day 6 as compared to the control, with the lowest virus titers in mice that received serum from the middle aged cohort (Fig. 6f). In this case the reduction in lung virus titers correlated well with the measured neutralization titers. For H4N8 the serum transfer slightly but significantly reduced virus titers on day 3. On day 6 post-infection the highest impact on virus titers was seen from the middle aged cohort sera (Fig. 6e, f). This reduction correlated with ELISA reactivity to H4, but not the findings in the neutralization assay. This indicates that these antibodies measured by ELISA mediate their effects via Fc-receptor mechanisms. Serum transfer also had a slight impact on H7N8 replication both on day 3 and day 6 but the reduction in lung virus titers never reached statistical significance (Fig. 6e, f). In summary we demonstrate that cross-reactive antibodies in the general human population are functional both through direct neutralizing activity as well as effector functions.

Discussion

It has been observed that infection with influenza viruses in humans induces immune responses of higher quality, quantity and longevity than influenza virus vaccination[6,7]. In recent years cross-reactive and cross-protective antibodies have become the focus of influenza research since they can guide efforts to design broadly protective influenza virus vaccines and therapeutics[31]. Here, we measured the antibody cross-reactome against an extensive panel of influenza virus HAs and NAs (including all know subtypes) induced by infection in animal models and in humans by ELISA. ELISAs are a very sensitive and useful tool to study antibody binding and cross-reactivity. However, they only provide limited insight into the biological activity of the measured responses. Using this technique we found significant differences in both breadth and magnitude of the antibody response in models commonly employed for influenza virus research.

For all animal models, the immune response against HAs was primarily focused on either group 1 (post H1N1 infection) or group 2 (post H3N2 infection). Anti-NA antibodies were mostly subtype specific. Mice and guinea pigs induced high antibody titers while the responses measured for ferrets were lower. Guinea pigs exhibited an exceptionally broad response compared to the other animal models. Ferrets had a low and relatively narrow immune response when assessed by ELISA even though they are capable of inducing high HI responses against homologous viruses. It has been noted that this HI response is usually focused on specific epitopes and is not reflective of the broad HI response of adult humans[32]. The extend of virus replication, which differs depending on virus strain and animal model, did not seem to be a major influence on cross-reactive antibody titers. The observed differences should be considered when choosing animal models for research on (universal) influenza virus vaccines since the model chosen might strongly influence the outcome of pre-clinical studies. Importantly, none of these models is accurately reflecting the immune response in human individuals with pre-existing immunity and complicated exposure histories against influenza virus. This highlights the need for human clinical trials for broadly protective/universal influenza virus vaccines.

In the human population, infection with influenza viruses induced significant antibody cross-reactivity both in terms of magnitude and breadth. The reactivity was narrow after H3N2 infection but surprisingly broad after pandemic H1N1 infection. Unexpectantly, the induction to group 2 HAs was almost as strong after pandemic H1N1 infection as after H3N2 infection (with the exception of the matched H3 HA). This phenomenon might be explained by the greater phylogenetic and antigenic distance between the pandemic H1N1 strain and the pre-pandemic seasonal H1N1 strains (especially the variable head domain of the HAs) to which humans have pre-existing immunity[33]. It has been noted before that pandemic H1N1 infection and vaccination induce anti-stalk antibodies in humans because they present a novel head domain to the immune system which then refocuses the antibody response towards the more conserved stalk domain to which memory exists[4,34,35]. However, the extent of this response was unknown so far. Also, an alternative hypothesis for this finding could be the low number of N-linked glycans on the HA of pH1N1 viruses as compare to the high number of N-linked glycans on the HA of current H3N2 viruses. While we cannot test this hypothesis in humans we did not find any clear evidence of an influence of the number of putative N-linked glycosylation sites of the subtrate HAs on the crossreactivity. Only small amounts of sera were available for these infected individuals, which prevented studying the functionality of these antibodies measured by ELISA. It is therefore not known whether the cross-group reactive antibodies elicited by infection are also functional *in vivo*. Another limitation of the study is that the ‘pre-infection’ serum samples were taken after onset of symptoms. The true pre-infection titers might therefore be even lower and the antibody induction even higher than reported here.

While high cross-reactive antibody titers were detected in humans after natural infection we wanted to further explore the breadth of the cross-reactome in the human population. This information is important since high baseline reactivity against a specific subtype could ameliorate disease and limit virus spread during a future pandemic with this subtype. We therefore studied the cross-reactome of the general human population by selecting 90 individuals from three different age groups (18–20, 33–44, 49–64) based on their putative influenza virus exposure history.

We found that the cross-reactivity profiles depend on the pre-exposure history and are influenced by the virus strains first encountered during childhood. The young cohort - who grew up when H1N1 and H3N2 viruses co-circulated - showed high reactivity to very recent isolates of these two subtypes with limited cross-reactivity. The middle-aged cohort who was first exposed to H3N2, had high titers to H3 and other group 2 HAs but low titers against H1 (which they only encountered later in life). Finally, the individuals in the experienced cohort were first exposed to H1N1 or H2N2 and exhibited very high titers to H2, H1 and related subtypes like H5. These findings provide evidence for the phenomenon in which the first HA subtype to which an individual is exposed leaves an immunological imprint that will heavily impact on the antibody cross-reactome that this person develops (also called original antigenic sin). The high cross-reactive group 1 HA titers in the experienced population might contribute to protection against new pandemic viruses that express group 1 HAs (like H5, H6 or others). In general we found that baseline antibody titers are low against H11, H12, H13 and others (group 1) and H7, H10 and H15 (group 2). Of note, H7,[36] and to some

extent also H10,[37] influenza viruses have recently infected humans in Asia with a high case fatality rate.

Importantly, these findings also translated into *in vitro* and *in vivo* functional assays. In a virus neutralization assay, we showed that the 33–44-year-old age group with the highest ELISA titers against H3 Phil82 also most effectively neutralized an H3N8 virus based on this HA. Similarly, the 18–20-year-old age group had high neutralizing titers against an H1N8 virus based on NC99, which is an HA from a strain that circulated during their childhood. Furthermore, these antibodies also conferred protection in an *in vivo* serum transfer model.

In conclusion, we have created antigenic landscapes that describe the antibody cross-reactome towards the influenza virus glycoproteins in animal models and humans recently infected with influenza viruses. We found that the prevalence and breadth of the antibody cross-reactome of the general human population varies largely and depends on the individual history of exposure to influenza viruses. These data provide important information for pandemic preparedness and the choice of animal models for the development of broadly protective influenza virus vaccines. Finally, the wide prevalence of cross-reactive antibodies in humans suggests that future universal vaccine strategies - targeting the HA head, stalk or NA - might be successful in boosting these antibody levels to protective titers.

Methods

Cells, viruses and proteins

Madin-Darby Canine Kidney (MDCK) cells and 293T Human Embryo Kidney cells were maintained in complete Dulbecco's Modified Eagle's Medium (cDMEM, Gibco) containing 10% fetal bovine serum (FBS, Gibco) and pen-strep mix (100 units/ml of penicillin and 100 μg/ml of streptomycin, Gibco). Influenza viruses were grown in 8–10 day old embryonated chicken eggs (Charles River Laboratories). Re-assortants were rescued using a previously described protocol[38]. A full list of viruses and abbreviations can be found in Supplementary Table 2. Sf9 cells were maintained in TNM-FH medium (Gemini Bio-Products) in the presence of 10% FBS and pen-strep mix. *BTI*-TN5B1-4 cells[39] were maintained in SFX medium (HyClone) containing Pen-strep mix. Recombinant proteins were expressed as described in detail before[13,40,41]. All HAs were expressed as ectodomains fused to a C-terminal fold on trimerization domain and a hexahistidine tag for purification. All NAs were expressed as ectodomains with an N-terminal hexahistidine tag and vasodilator-stimulated phosphoprotein tetramerization domain. The design of the constructs were identical to designs described by the Wilson laboratory at Scripps to produce high quality recombinant HAs and NAs for crystallographic studies[42,43]. All proteins were purified using Standard Operation Procedures (SOPs) that have been established in the laboratory to guarantee consistent quality of the recombinant proteins[41]. A list with recombinant HA and NA proteins used in this study can be found in Supplementary Table 3.

Animal infections

All of the animal experiments described here were conducted by using protocols approved by the Icahn School of Medicine at Mount Sinai Institutional Animal Care and Use Committee. Infections and blood draws were performed under ketamine/xylazine anesthesia in all animals. Ferrets received 0.45 ml of ketamine/xylazine mix intramuscularly, guinea pigs received 200 l of 30 mg/kg of ketamine and 5 mg/kg of xylazine intramuscularly and mice received 0.1 ml of 0.15 mg/kg of ketamine and 0.03 mg/kg of xylazine intraperitoneally. Animals were sequentially infected with sublethal doses of two divergent viruses of the same subtype 6 weeks apart. For H1N1, the first infection was performed with A/New Caledonia/20/99 (1×10^5 PFU per mouse in 50 μl, n=10; 1×10^6 PFU per guinea pig in 300 μl, n=3; 1×10^6 PFU per ferret in 1000 μl, n=2) followed by an infection with A/California/04/09 (1×10^4 PFU per mouse in 50 μl; 1×10^6 PFU per guinea pig in 300 μl; 1×10^6 PFU per ferret in 1000 μl). For H3N2, the first infection was performed with A/Philippines/2/82 (1×10^5 PFU per mouse in 50 μl, n=10; 1×10^6 PFU per guinea pig in 300 μl, n=3; 1×10^6 PFU per ferret in 1000 μl, n=2) followed by A/Victoria/361/11 (5×10^5 PFU per mouse in 50 μl; 1×10^6 PFU per guinea pig in 300 μl; 1×10^6 PFU per ferret in 1000 μl). Sera were collected on day 42 (post first infection) and day 84 (post second infection). Serum pools of naïve animals were used to establish background reactivity in ELISA. Samples for ferrets and guinea pigs were analyzed individually and geometric mean titers reported. Serum of one guinea pig of the repeated H3N2 infection group could not be used and geometric mean titers of the remaining two animals were reported. Mouse samples for each time point and group were pooled and analysis was performed in technical duplicates.

Serum samples from influenza A virus infected individuals

Clinical-epidemiological data along with a blood samples were collected after informed written consent was obtained under protocol 11–116, reviewed and approved by the Scientific Ethics Committee of the School of Medicine at Pontificia Universidad Católica de Chile prior to the start of sample collection. Matched human sera samples, from days 1 and 21 or 28 post infection (d.p.i.), were obtained and archived from 19 hospitalized patients infected with human influenza A virus (IAV) between years 2011 and 2013 in Santiago, Chile (Supplementary Table 1). All samples were de-identified of any personal information prior to blinded analysis (IRB exempt, HS#: 1500125). IAV infection was confirmed by qRT-PCR of viral RNA extracted from nasopharyngeal samples by the Clinical Virology Laboratory at Pontificia Universidad Católica de Chile (PUC). Positive samples were subtyped as H1N1pdm09 or H3N2 influenza A strains by qRT-PCR analysis and/or confirmed by hemagglutinin inhibition (HI) assays. Serum volumes for 2 patients were not sufficient to complete all testing. For p3/2011 (pH1N1) reactivity to N8 and H3 HK68 could not be tested. For p36/2012 reactivity to H2 Jap57, H3 seMass11, H10, H11, H12, H13, H16, H18, cH5/3, N1 Texa91, N2 Vic11, N2 Sing57, N3, N4, N5, N6, N7, N9, N10 and B NA could not be tested.

Human cohort sera

90 human serum samples were ordered as research reagents from Innovative Research (Michigan, USA). The individuals were chosen to fall within 3 separate age groups (18–20, 33–44, 49–64 years old) and to obtain similar male/female ratios for each group (Supplementary Table 4). All samples were collected between August and November 2014 and were received de-identified except for age, race and sex.

Enzyme linked immunosorbent assay (ELISA)

ELISAs were performed as previously described[25]. In short, 96-well high-binding, flat-bottom plates were coated with 50 µl/well of recombinant protein at a concentration of 2 µg/ml in coating buffer (50 mM sodium carbonate, 50 mM sodium hydrogen carbonate, pH 9.4) and incubated overnight at 4 °C. Coating buffer was removed and plates were incubated for 1 hour at 25 °C with 220 µl of blocking solution (mouse: PBS + 0.5% Tween-20 + 3% milk powder; human, ferret, guinea pig: PBS + 0.5% Tween-20 + 3% goat serum + 0.5% milk powder). Sera were 3-fold serially diluted in blocking solution and plates were incubated for two hours at 25 °C. Plates were washed three times with PBS-T (PBS + 0.5% Tween-20) and 50 µl of IgG-specific secondary antibody diluted in blocking solution added to each well (mouse: 1:3000, Sigma #A9044; ferret: 1:5000, Alpha Diagnostic International #70530; guinea pig: 1:3000, Millipore #AP108P; human: 1:3000, Sigma #A0293). After one hour of incubation at 25 °C, plates were washed 3 times with PBS-T. Plates were developed with 100 µl of SigmaFast OPD (Sigma) and stopped after 10 min by addition of 3M hydrochloric acid. Plates were then read at a wavelength of 490 nm. For mice, guinea pigs and ferrets, the cut-off for endpoint titers was calculated as the mean and 3 standard deviations of all blank wells. For human samples, a standard cut-off of 0.07 was used. Plates were discarded if the background and 3 standard deviations exceeded the standard cut-off.

Microneutralization assay

For increased sensitivity - without unspecific inhibition of viruses by other serum proteins – IgG from human cohort sera were purified with protein G columns and reconstituted to the original serum volume in PBS. MDCK cells were seeded in 96-well tissue culture plates at a density of $1.5–1.8 \times 10^4$ cells/well in 100 µl of cDMEM and incubated at 37 °C overnight. IgG were 2-fold serially diluted in infection media (minimal essential media containing tosyl phenylalanyl chloromethyl ketone treated trypsin at a concentration of 1 µg/ml) starting with a 1:2 dilution. 50 µl of serially diluted IgG were incubated for one hour at 25 °C with 50 µl of virus diluted to 200 plaque forming units per 50 µl. Cells were washed once with PBS, 100 µl of virus antibody mixture was transferred to each well and plates were incubated at 37 °C for one hour. Cells were washed once with PBS and 50 µl of serially diluted antibody at the original concentration, as well as 50 µl of infection media were added to each well. Plates were incubated for 48–72 h and read by hemagglutination assay. Wells containing virus only without antibodies served as positive control.

Serum transfer experiments in mice

Serum samples from each age group were pooled separately and sterile filtrated. Commercially available immunoglobulin-depleted human serum (BBI Solutions,

#SF5050-2) was used as negative control. For each virus tested, 10 mice per serum group were injected intraperitoneally with 250 μl of serum. Two hours later, mice were infected intranasally under ketamine/xylazine anesthesia with 10^5 PFU of virus in 50 μl (diluted in PBS). Five mice each per serum group were euthanized on day three and day six post infection. Lungs were extracted, homogenized in 600 μl of PBS and the cell debris removed by centrifugation. Aliquots were stored at −80 °C until the viruses were titered by plaque assay as previously described[25].

Graphical representations

All data graphs, except for the 3D antibody landscapes, were generated in GraphPad Prism 7. To visualize antibody titers of human serum samples against different HA subtypes, 3D antibody landscapes[44] were constructed. In the antibody landscapes, the relative distance in the horizontal plane (*x*-*y* coordinates) represents the amino acid sequence distance among strains, and height (*z*-coordinate) represents the geometric mean antibody titers against corresponding strains on the horizontal plane. The horizontal plane was constructed by multi-dimensional scaling of the amino acid sequence distance[45,46]. The sequence distances among strains were defined as the total numbers of different amino acids between corresponding HAs in the multiple sequence alignment of all the HAs used in this study. The sum of squared errors between the Euclidean distance in the 2D plane and the HA sequence distance was minimized by the SMACOF algorithm[46]. The HA sequences were divided into two HA groups, one of which contains H1, H2, H5, H6, H8, H9, H11, H12, H13, H16, H17 and H18 and the other contains H3, H4, H7, H10, H14, and H15. For each HA group, the surface of antibody landscape was approximated from geometric mean antibody titers using multilevel B-splines. We used the mba.surf function implemented in the Multilevel B-spline Approximation package in R version 3.2.5. Interactive 3D figures are available as online supplementary materials.

Statistical analysis

Statistical analysis was performed with GraphPad Prism 7. Microneutralization titers were compared with ordinary one-way ANOVAs followed by Tukey's multiple comparisons tests. The viral lung titers were compared with ordinary one-way ANOVAs followed by Dunnett's multiple comparison tests with the no-Ig group serving as the control group. The nonlinear regression function "Plateau followed by one phase decay" was used to create nonlinear fit curves for the ELISA data.

Supplementary Material

Refer to Web version on PubMed Central for supplementary material.

Acknowledgments

We thank L. Aguado (Icahn School of Medicine at Mount Sinai) for cloning of several of the HA expression vectors, J. Runstadler (MIT) for making several avian influenza viruses available to us, F. Amanat for IgG purification and P. E. Leon for providing us with the H3N8 and H9N4 virus used in this study. We would also like to thank C. Marizzi at the Cold Spring Harbor Laboratory DNA Learning Center (DNALC) for reviewing the manuscript. This project was partially supported by the NIH Centers of Excellence in Influenza virus Research and Surveillance (CEIRS, contract number HHSN272201400008C to A.G.S., P.P., F.K., R.A.M. and N.M.B.), U19 AI109946-01 (to P.P. and F.K.) and R01 AI117287-01A1 (to F.K. and N.M.B.). R.A.M. was supported by

CONICYT Fondecyt grants 1121172 and 1161791, Proyecto Anillo CONICYT PIA ACT 1408 and by the Program Iniciativa Científica Milenio from the Chilean Ministry of Economy, Development and Tourism grant P09/016-F. We also thank BEI Resources for providing influenza virus HA and NA sequences and R. Fouchier (Erasmus MC, The Netherlands) for generously depositing HA and NA plasmids at this resource.

References

1. Jayasundara K, Soobiah C, Thommes E, Tricco AC, Chit A. Natural attack rate of influenza in unvaccinated children and adults: a meta-regression analysis. BMC Infect Dis. 2014; 14:670. [PubMed: 25495228]
2. Krammer F, Palese P. Advances in the development of influenza virus vaccines. Nat Rev Drug Discov. 2015; 14:167–182. DOI: 10.1038/nrd4529 [PubMed: 25722244]
3. Horimoto T, Kawaoka Y. Influenza: lessons from past pandemics, warnings from current incidents. Nat Rev Microbiol. 2005; 3:591–600. DOI: 10.1038/nrmicro1208 [PubMed: 16064053]
4. Wrammert J, et al. Broadly cross-reactive antibodies dominate the human B cell response against 2009 pandemic H1N1 influenza virus infection. J Exp Med. 2011; 208:181–193. jem.20101352 [pii]. DOI: 10.1084/jem.20101352 [PubMed: 21220454]
5. Pica N, et al. Hemagglutinin stalk antibodies elicited by the 2009 pandemic influenza virus as a mechanism for the extinction of seasonal H1N1 viruses. Proc Natl Acad Sci U S A. 2012; 109:2573–2578. 1200039109 [pii]. DOI: 10.1073/pnas.1200039109 [PubMed: 22308500]
6. Margine I, et al. H3N2 influenza virus infection induces broadly reactive hemagglutinin stalk antibodies in humans and mice. J Virol. 2013; 87:4728–4737. DOI: 10.1128/JVI.03509-12 [PubMed: 23408625]
7. Yu X, et al. Neutralizing antibodies derived from the B cells of 1918 influenza pandemic survivors. Nature. 2008; 455:532–536. DOI: 10.1038/nature07231 [PubMed: 18716625]
8. Ohmit SE, Petrie JG, Cross RT, Johnson E, Monto AS. Influenza hemagglutination-inhibition antibody titer as a correlate of vaccine-induced protection. J Infect Dis. 2011; 204:1879–1885. DOI: 10.1093/infdis/jir661 [PubMed: 21998477]
9. Heaton NS, Sachs D, Chen CJ, Hai R, Palese P. Genome-wide mutagenesis of influenza virus reveals unique plasticity of the hemagglutinin and NS1 proteins. Proc Natl Acad Sci U S A. 2013; 110:20248–20253. DOI: 10.1073/pnas.1320524110 [PubMed: 24277853]
10. Yewdell JW, Webster RG, Gerhard WU. Antigenic variation in three distinct determinants of an influenza type A haemagglutinin molecule. Nature. 1979; 279:246–248. [PubMed: 86955]
11. Wohlbold TJ, Krammer F. In the shadow of hemagglutinin: a growing interest in influenza viral neuraminidase and its role as a vaccine antigen. Viruses. 2014; 6:2465–2494. DOI: 10.3390/v6062465 [PubMed: 24960271]
12. Yang X, et al. A Beneficiary Role for Neuraminidase in Influenza Virus Penetration through the Respiratory Mucus. PLoS One. 2014; 9:e110026. [PubMed: 25333824]
13. Wohlbold TJ, et al. Vaccination with Adjuvanted Recombinant Neuraminidase Induces Broad Heterologous, but Not Heterosubtypic, Cross-Protection against Influenza Virus Infection in Mice. MBio. 2015; 6
14. Easterbrook JD, et al. Protection against a lethal H5N1 influenza challenge by intranasal immunization with virus-like particles containing 2009 pandemic H1N1 neuraminidase in mice. Virology. 2012; 432:39–44. S0042-6822(12)00288-7 [pii]. DOI: 10.1016/j.virol.2012.06.003 [PubMed: 22727831]
15. Ekiert DC, et al. Antibody recognition of a highly conserved influenza virus epitope. Science. 2009; 324:246–251. 1171491 [pii]. DOI: 10.1126/science.1171491 [PubMed: 19251591]
16. Ekiert DC, et al. A highly conserved neutralizing epitope on group 2 influenza A viruses. Science. 2011; 333:843–850. science.1204839 [pii]. DOI: 10.1126/science.1204839 [PubMed: 21737702]
17. Sui J, et al. Structural and functional bases for broad-spectrum neutralization of avian and human influenza A viruses. Nat Struct Mol Biol. 2009; 16:265–273. nsmb.1566 [pii]. DOI: 10.1038/nsmb.1566 [PubMed: 19234466]
18. Dreyfus C, et al. Highly conserved protective epitopes on influenza B viruses. Science. 2012; 337:1343–1348. science.1222908 [pii]. DOI: 10.1126/science.1222908 [PubMed: 22878502]

19. Jegaskanda S, Weinfurter JT, Friedrich TC, Kent SJ. Antibody-dependent cellular cytotoxicity is associated with control of pandemic H1N1 influenza virus infection of macaques. J Virol. 2013; 87:5512–5522. DOI: 10.1128/JVI.03030-12 [PubMed: 23468501]
20. Jegaskanda S, et al. Cross-reactive influenza-specific antibody-dependent cellular cytotoxicity antibodies in the absence of neutralizing antibodies. J Immunol. 2013; 190:1837–1848. DOI: 10.4049/jimmunol.1201574 [PubMed: 23319732]
21. Laidlaw BJ, et al. Cooperativity between CD8+ T cells, non-neutralizing antibodies, and alveolar macrophages is important for heterosubtypic influenza virus immunity. PLoS Pathog. 2013; 9:e1003207. [PubMed: 23516357]
22. DiLillo DJ, Palese P, Wilson PC, Ravetch JV. Broadly neutralizing anti-influenza antibodies require Fc receptor engagement for in vivo protection. J Clin Invest. 2016; 126:605–610. DOI: 10.1172/JCI84428 [PubMed: 26731473]
23. Terajima M, et al. Complement-dependent lysis of influenza a virus-infected cells by broadly cross-reactive human monoclonal antibodies. J Virol. 2011; 85:13463–13467. DOI: 10.1128/JVI.05193-11 [PubMed: 21994454]
24. Dilillo DJ, Tan GS, Palese P, Ravetch JV. Broadly neutralizing hemagglutinin stalk-specific antibodies require FcγR interactions for protection against influenza virus in vivo. Nat Med. 2014; 20:143–151. DOI: 10.1038/nm.3443 [PubMed: 24412922]
25. Nachbagauer R, et al. Induction of broadly reactive anti-hemagglutinin stalk antibodies by an H5N1 vaccine in humans. J Virol. 2014; 88:13260–13268. DOI: 10.1128/JVI.02133-14 [PubMed: 25210189]
26. Henry Dunand CJ, et al. Both Neutralizing and Non-Neutralizing Human H7N9 Influenza Vaccine-Induced Monoclonal Antibodies Confer Protection. Cell Host Microbe. 2016; 19:800–813. DOI: 10.1016/j.chom.2016.05.014 [PubMed: 27281570]
27. Krause JC, et al. Human Monoclonal Antibodies to Pandemic 1957 H2N2 and Pandemic 1968 H3N2 Influenza Viruses. J Virol. 2012; 86:6334–6340. JVI.07158-11 [pii]. DOI: 10.1128/JVI.07158-11 [PubMed: 22457520]
28. Smith G, et al. Origins and evolutionary genomics of the 2009 swine-origin H1N1 influenza A epidemic. Nature. 2009; 459:1122–1125. [PubMed: 19516283]
29. Krammer F, Palese P. Universal influenza virus vaccines: need for clinical trials. Nat Immunol. 2014; 15:3–5. DOI: 10.1038/ni.2761 [PubMed: 24352315]
30. Miller MS, et al. Neutralizing Antibodies Against Previously Encountered Influenza Virus Strains Increase over Time: A Longitudinal Analysis. Sci Transl Med. 2013; 5:198ra107.
31. Krammer F, Palese P. Influenza virus hemagglutinin stalk-based antibodies and vaccines. Curr Opin Virol. 2013; 3:521–530. DOI: 10.1016/j.coviro.2013.07.007 [PubMed: 23978327]
32. Li Y, et al. Immune history shapes specificity of pandemic H1N1 influenza antibody responses. J Exp Med. 2013; 210:1493–1500. DOI: 10.1084/jem.20130212 [PubMed: 23857983]
33. Garten R, et al. Antigenic and genetic characteristics of swine-origin 2009 A(H1N1) influenza viruses circulating in humans. Science. 2009; 325:197–201. [PubMed: 19465683]
34. Li GM, et al. Pandemic H1N1 influenza vaccine induces a recall response in humans that favors broadly cross-reactive memory B cells. Proc Natl Acad Sci U S A. 2012; 109:9047–9052. 1118979109 [pii]. DOI: 10.1073/pnas.1118979109 [PubMed: 22615367]
35. Pica N, et al. Hemagglutinin stalk antibodies elicited by the 2009 pandemic influenza virus as a mechanism for the extinction of seasonal H1N1 viruses. Proc Natl Acad Sci U S A. 2012; 109:2573–2578. 1200039109 [pii]. DOI: 10.1073/pnas.1200039109 [PubMed: 22308500]
36. Gao R, et al. Human infection with a novel avian-origin influenza A (H7N9) virus. N Engl J Med. 2013; 368:1888–1897. DOI: 10.1056/NEJMoa1304459 [PubMed: 23577628]
37. Chen H, et al. Clinical and epidemiological characteristics of a fatal case of avian influenza A H10N8 virus infection: a descriptive study. Lancet. 2014; 383:714–721. DOI: 10.1016/S0140-6736(14)60111-2 [PubMed: 24507376]
38. Martínez-Sobrido L, García-Sastre A. Generation of recombinant influenza virus from plasmid DNA. J Vis Exp. 2010
39. Krammer F, et al. Trichoplusia ni cells (High Five) are highly efficient for the production of influenza A virus-like particles: a comparison of two insect cell lines as production platforms for

influenza vaccines. Mol Biotechnol. 2010; 45:226–234. DOI: 10.1007/s12033-010-9268-3 [PubMed: 20300881]

40. Krammer F, et al. A carboxy-terminal trimerization domain stabilizes conformational epitopes on the stalk domain of soluble recombinant hemagglutinin substrates. PLoS One. 2012; 7:e43603. PONE-D-12-16229 [pii]. [PubMed: 22928001]
41. Margine I, Palese P, Krammer F. Expression of Functional Recombinant Hemagglutinin and Neuraminidase Proteins from the Novel H7N9 Influenza Virus Using the Baculovirus Expression System. J Vis Exp. 2013
42. Xu X, Zhu X, Dwek RA, Stevens J, Wilson IA. Structural characterization of the 1918 influenza virus H1N1 neuraminidase. J Virol. 2008; 82:10493–10501. JVI.00959-08 [pii]. DOI: 10.1128/JVI.00959-08 [PubMed: 18715929]
43. Stevens J, et al. Structure of the uncleaved human H1 hemagglutinin from the extinct 1918 influenza virus. Science. 2004; 303:1866–1870. 1093373 [pii]. DOI: 10.1126/science.1093373 [PubMed: 14764887]
44. Fonville JM, et al. Antibody landscapes after influenza virus infection or vaccination. Science. 2014; 346:996–1000. DOI: 10.1126/science.1256427 [PubMed: 25414313]
45. Ito K, et al. Gnarled-trunk evolutionary model of influenza A virus hemagglutinin. PLoS One. 2011; 6:e25953. [PubMed: 22028800]
46. Borg, I., Groenen, P. Modern Multidimensional Scaling:Theory and Applications. Springer; 2005.

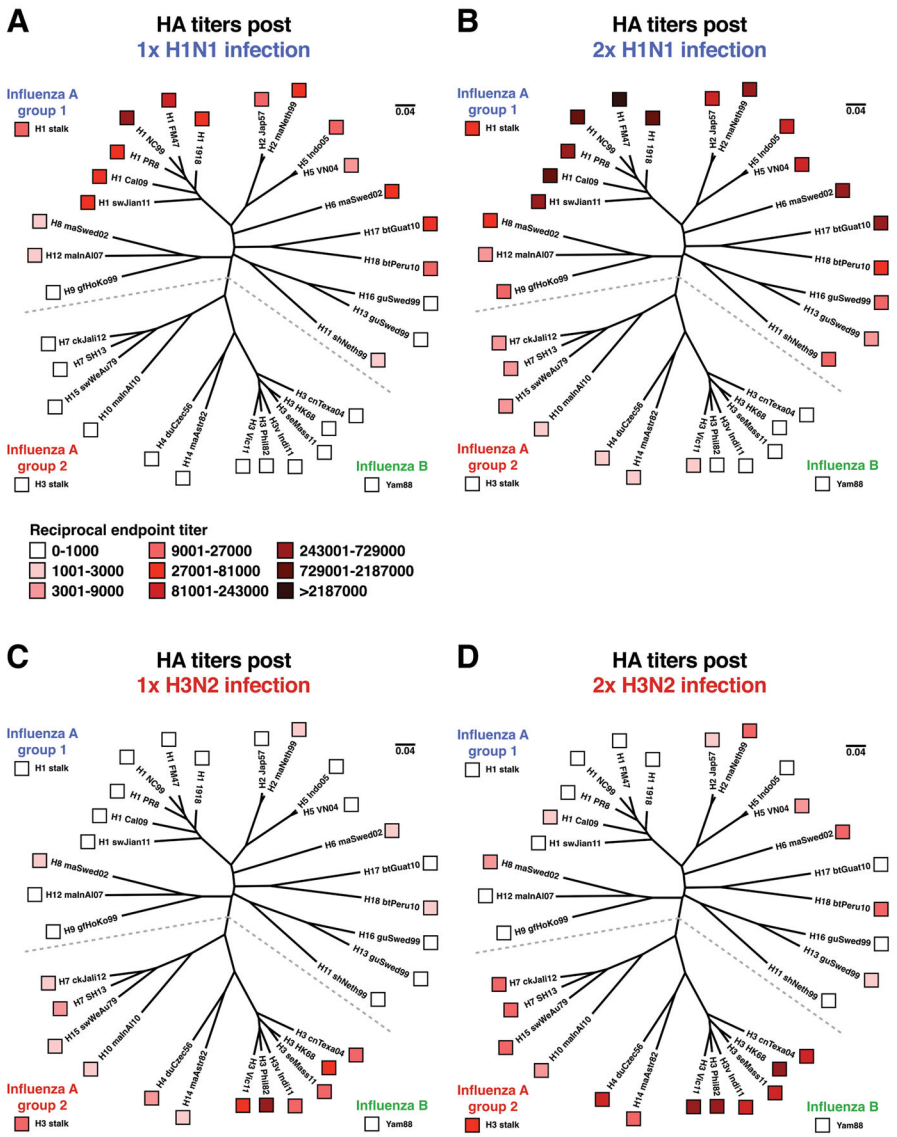

Figure 1. Cross-reactive HA antibody responses in the mouse model measured by ELISA

Serum IgG antibodies against all subtypes of HA were measured by ELISA. Pooled sera of 10 mice per group were measured in technical duplicates and the geometric mean value was used for graphical representation. A heat map overlay on top of a phylogenetic tree was used to illustrate the antibody titers induced by repeated influenza virus infection. The scale bar represents 4% amino acid difference. **A)** HA titers after a single H1N1 (NC99) infection in mice. **B)** HA titers after two consecutive H1N1 (NC99+NL09) infections in mice. **C)** HA titers after a single H3N2 (Phil82) infection in mice. **D)** HA titers after two consecutive H3N2 (Phil82+Vic11) infections in mice.

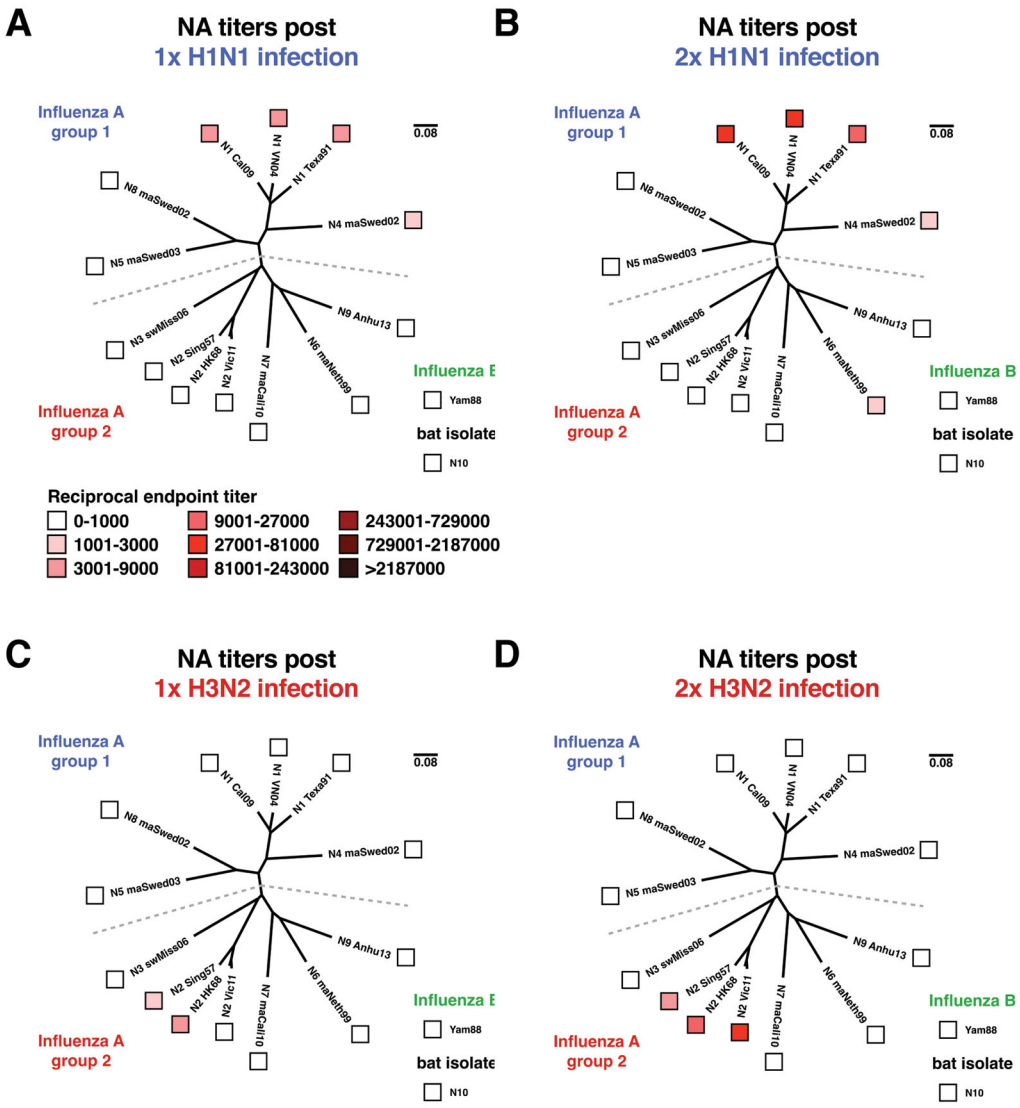

Figure 2. Cross-reactive NA antibody responses in the mouse model measured by ELISA

Serum IgG antibodies against NA were measured by ELISA. Pooled sera of 10 mice per group were measured in technical duplicates and the geometric mean value was used for graphical representation. A heat map overlay on top of a phylogenetic tree was used to illustrate the antibody titers induced by repeated influenza virus infection. The scale bar represents 8% amino acid difference. **A)** NA titers after a single H1N1 (NC99) infection in mice. **B)** NA titers after two consecutive H1N1 (NC99+NL09) infections in mice. **C)** NA titers after a single H3N2 (Phil82) infection in mice. **D)** NA titers after two consecutive H3N2 (Phil82+Vic11) infections in mice.

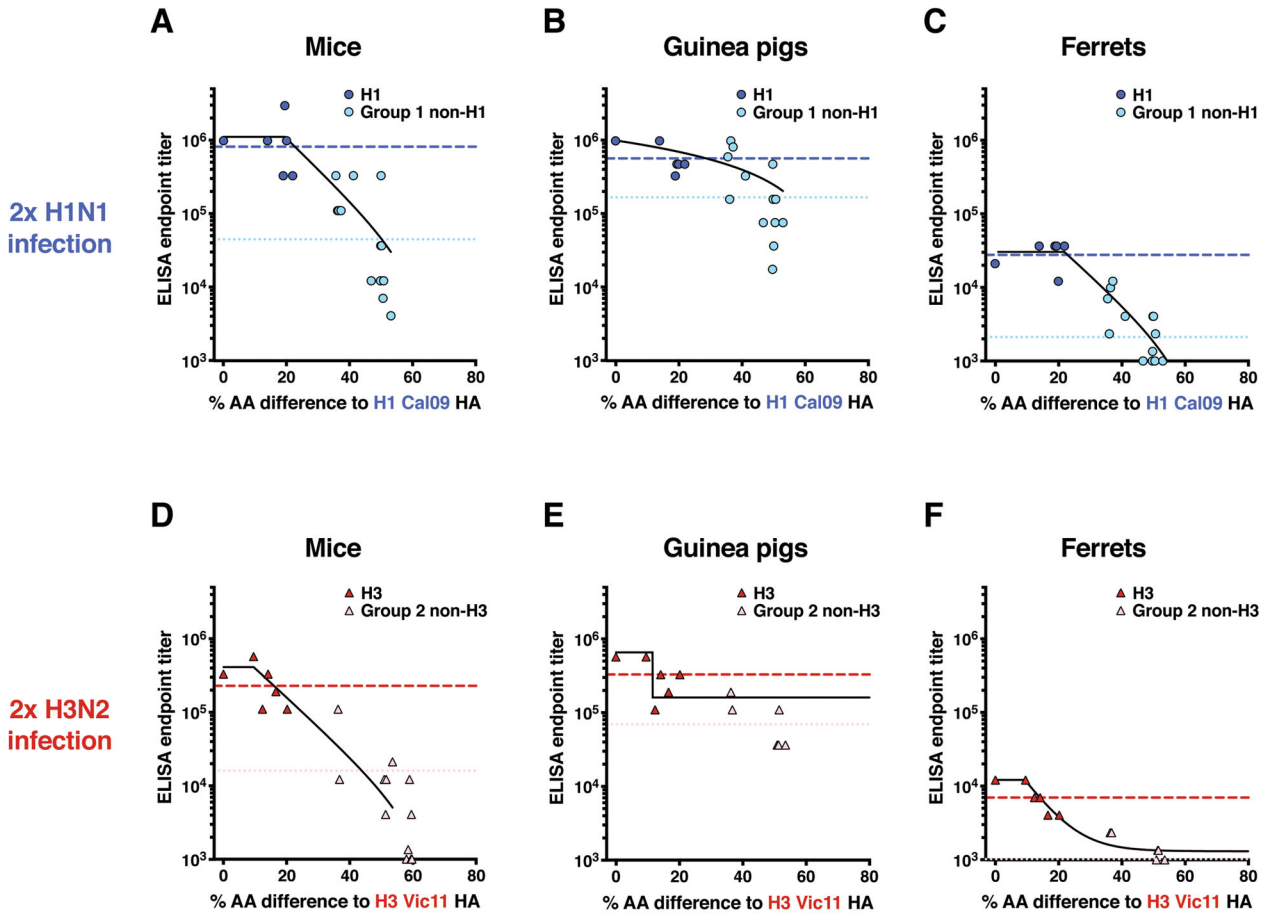

Figure 3. Cross-reactive antibody titers post infection negatively correlate with phylogenetic distance

To illustrate a correlation of antibody titers with phylogenetic distance, antibody titers measured by ELISA after sequential influenza virus infection were plotted on the *y*-axis and the percent amino acid difference to the HA of the strain used for the second infection was plotted on the *x*-axis. Each point represents the geometric mean titer measured against a single HA (dark blue dot for H1 HAs, light blue dot for other group 1 HAs, dark red triangle for H3 HAs, light red triangle for other group 2 HAs). A non-linear fit (plateau followed by one phase decay) was performed to illustrate the differences in the breadth of the antibody response in all animals. Points for HAs with titers lower than 10^3 are plotted at 10^3. The geometric mean titer against all non-H1 group 1 HAs is plotted as a light blue line. The geometric mean titer against all non-H3 group 2 HAs is plotted as a light red line. **A)** Mouse group 1 HA titers after two consecutive H1N1 (NC99+NL09) infections. ELISAs were performed on pooled sera of 10 mice and geometric mean titers of technical duplicates are shown. **B)** Guinea pig group 1 HA titers after two consecutive H1N1 (NC99+NL09) infections. ELISAs were performed on individual sera of 3 guinea pigs and geometric mean titers are shown. **C)** Ferret group 1 HA titers after two consecutive H1N1 (NC99+NL09) infections. ELISAs were performed on individual sera of 2 ferrets and geometric mean titers are shown. **D)** Mouse group 2 HA titers after two consecutive H3N2 (Phil82+Vic11) infections. ELISAs were performed on pooled sera of 10 mice and geometric mean titers of

technical duplicates are shown. **E)** Guinea pig group 2 HA titers after two consecutive H3N2 (Phil82+Vic11) infections. ELISAs were performed on individual sera of 2 guinea pigs and geometric mean titers are shown. **F** Ferret group 2 HA titers after two consecutive H3N2 (Phil82+Vic11) infections. ELISAs were performed on individual sera of 2 ferrets and geometric mean titers are shown.

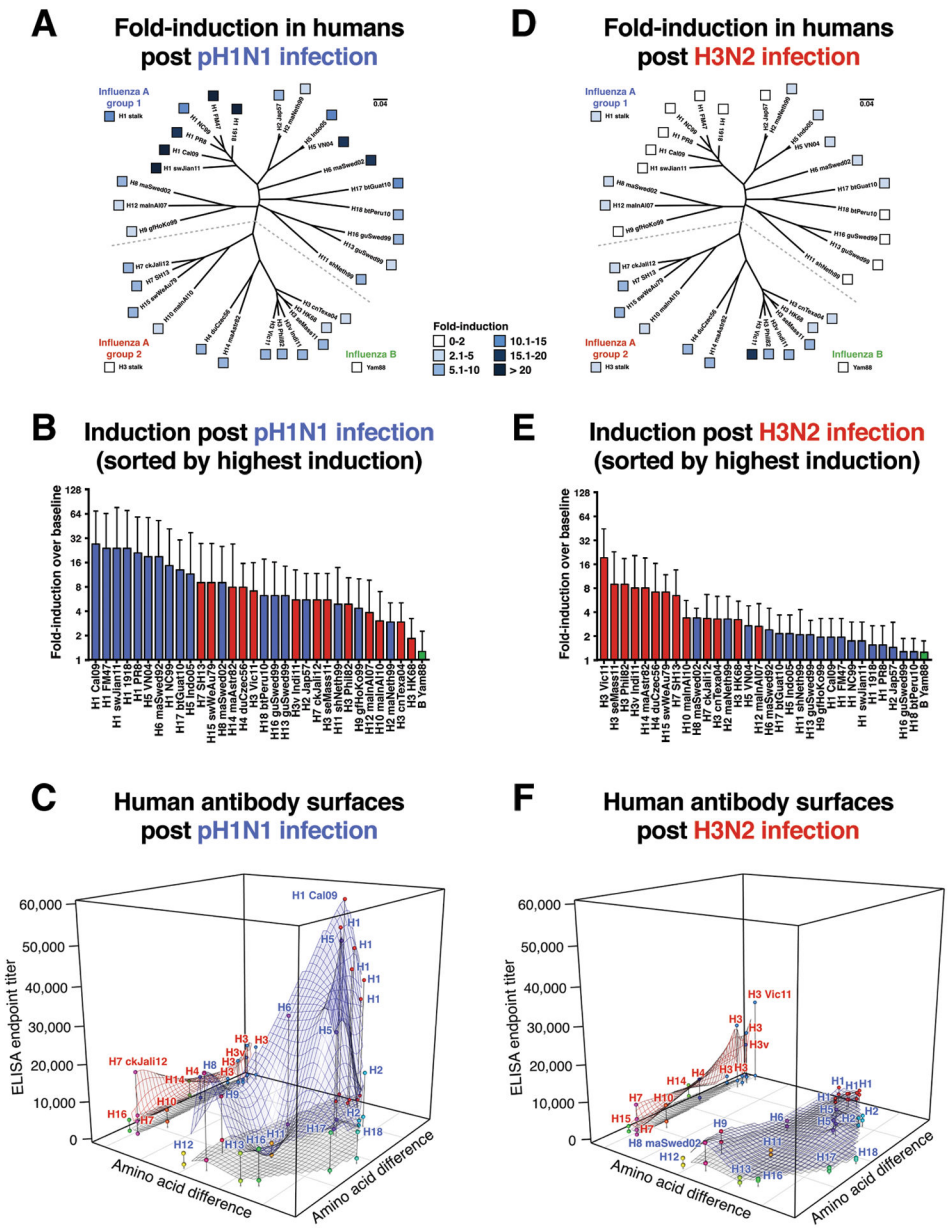

Figure 4. Human antibody responses post pH1N1 infection are broader than post H3N2 infection

A) Geometric mean fold-induction of individual antibody responses (n=9) post pH1N1 infection was plotted as a heat-map on a phylogenetic tree of HA. The scale bar represents 4% amino acid difference. **B)** The geometric mean fold-induction and 95% confidence intervals post pH1N1 infection of 9 individuals was plotted in a bar graph and sorted from highest to lowest induction. Group 1 HAs are shown as blue bars, group 2 HAs are shown as red bars and influenza B HA is shown in green. **C)** Three dimensional surfaces of the pre- and post-pH1N1 infection antibody titers were generated by plotting the relative distances of HAs to each other based on amino acid differences. Both *x*-and *y*-axes show amino acid differences and geometric mean titers (n=9) are plotted on the *z*-axis. The post-infection surfaces were plotted in color (blue for group 1 HAs, red for group 2 HAs) and the

corresponding pre-infection surfaces are plotted in gray. **D)** Geometric mean fold-induction of individual antibody responses (n=10) post H3N2 infection was plotted as a heat-map on a phylogenetic tree of HA. The scale bar represents 8% amino acid difference. **E)** The geometric mean fold-induction and 95% confidence intervals post H3N2 infection of 10 individuals was plotted in a bar graph and sorted from highest to lowest induction. Group 1 HAs are shown as blue bars, group 2 HAs are shown as red bars and influenza B HA is shown in green. **F)** Three dimensional surfaces of the pre- and post-H3N2 infection antibody titers were generated by plotting the relative distances of HAs to each other based on amino acid differences. Both *x*-and *y*-axes show amino acid differences and geometric mean titers (n=10) are plotted on the *z*-axis. The post-infection surfaces were plotted in color (blue for group 1 HAs, red for group 2 HAs) and the corresponding pre-infection surfaces are plotted in gray.

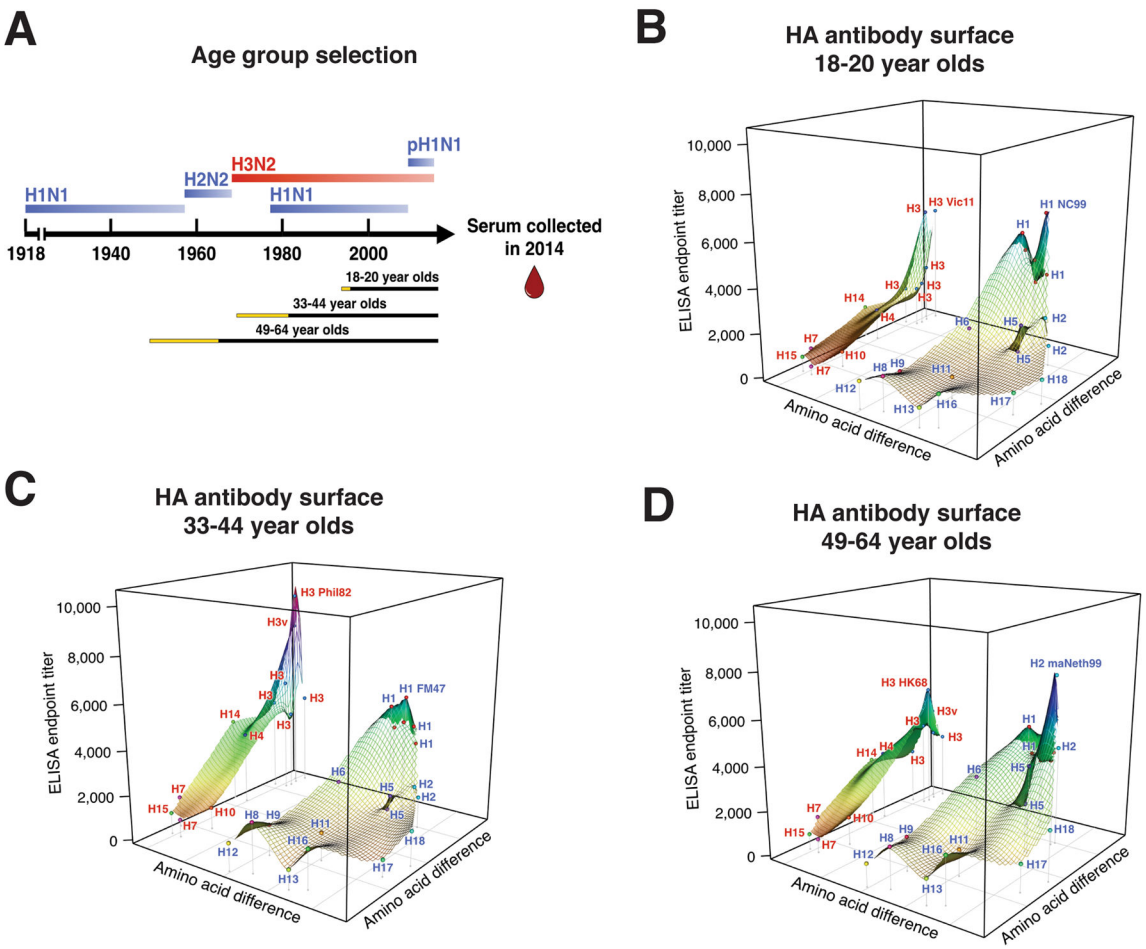

Figure 5. Titers in the general human population show distinct age related patterns

A) Schematic of selection of age groups that were tested. To investigate the effect of pre-exposure to different viruses, three distinct age groups were selected depending on the influenza viruses that most likely circulated during the childhood of the individuals. The oldest age group (49–64 year olds, 'experienced') was born when either a drifted version of the 1918 H1N1 virus or the H2N2 pandemic virus circulated. All individuals in this group should therefore have had exposure to H2N2 viruses. The slightly younger age group (33–44 year olds, 'middle-aged') was born after H2N2 went extinct and was replaced by the group 2 H3N2 virus and has therefore not been previously exposed to H2N2. 18–20 year olds ('young' cohort) were used as a young control group with only a limited exposure to group 1 and group 2 influenza A virus strains. **B–D)** To illustrate the differences of antibody profiles in the different age groups, three dimensional antigenic landscapes were plotted. All HAs are shown in their relative difference to each other based on amino acid sequences on the *x*- and *y*-axes. The geometric mean titers were plotted on the *z*-axis. **B)** Geometric mean titers of 18–20 year old individuals (n=30). **C)** Geometric mean titers of 33–44 year old individuals (n=30). **D)** Geometric mean titers of 49–64 year old individuals (n=30).

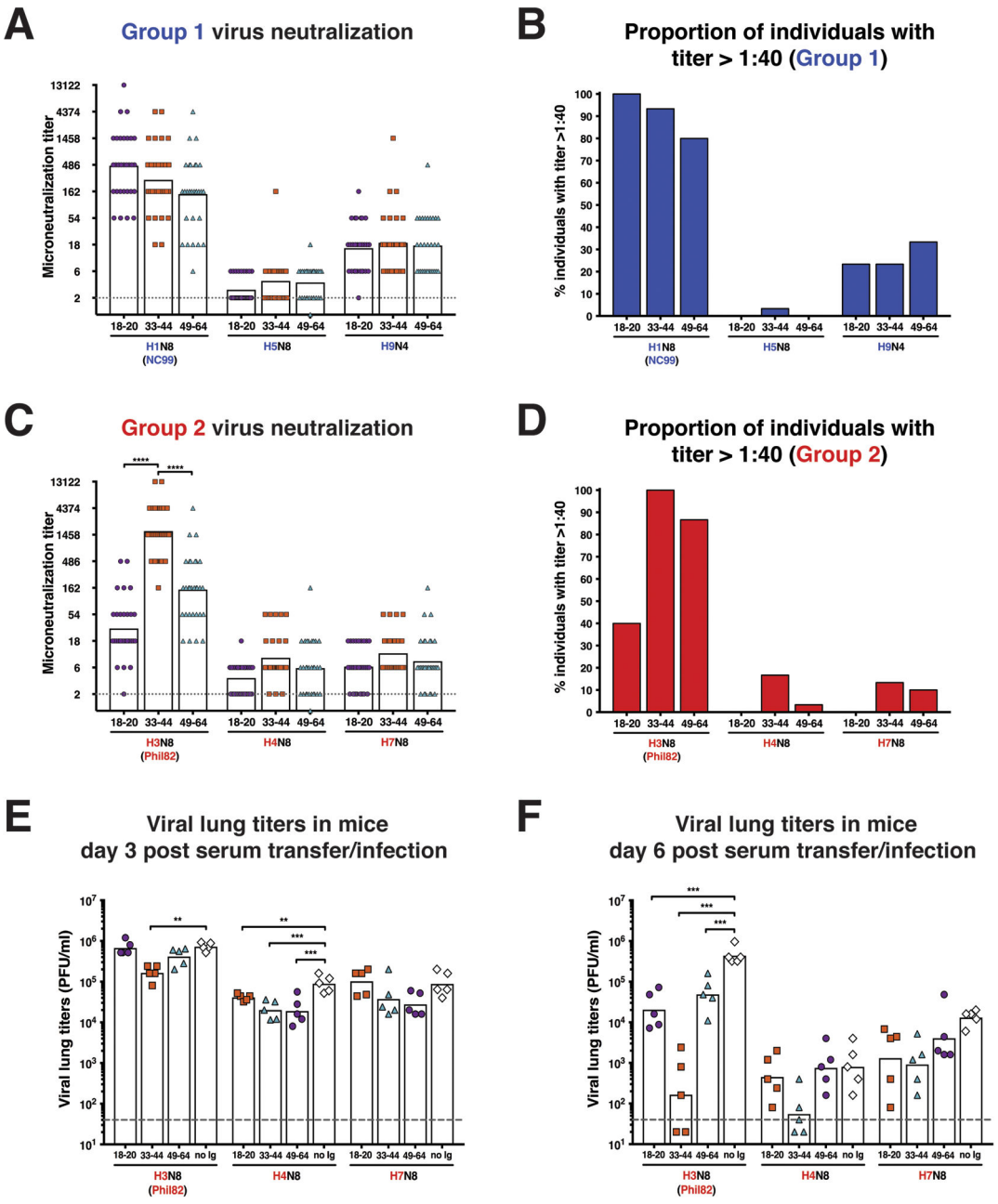

Figure 6. *In vitro* and *in vivo* protective effect of sera from the general human population

To test if antibody titers measured by ELISA also translate to measurable neutralizing responses *in vitro* and protective responses *in vivo*, re-assortant viruses that contain the same PR8 backbone and an irrelevant neuraminidase were generated for H1, H3, H4, H4, H7 and H9. **A)** Individual microneutralization titers against group 1 viruses (H1, H5, H9) are shown for sera from 18–20 year olds (blue dots, n=30), 33–44 year olds (red squares, n=30) and 49–64 year olds (teal triangles, n=30). A bar that represents the geometric mean titer is shown for each group. The gray line indicates the limit of detection for the assay. For each virus, groups were compared with an ordinary one-way ANOVA, followed by a Tukey's

multiple comparisons test. Statistical significance is indicated as follows: ** = $p \leq 0.01$, *** = $p \leq 0.001$, **** = $p \leq 0.0001$. **B)** Proportion of individuals with a neutralization titer of 1:40 or higher against group 1 viruses (H1, H5, H9) for each age group (n=30 per group). **C)** Individual microneutralization titers against group 2 viruses (H3, H4, H7) are shown for sera from 18–20 year olds (blue dots, n=30), 33–44 year olds (red squares, n=30) and 49–64 year olds (teal triangles, n=30). A bar that represents the geometric mean titer is shown for each group. The gray line indicates the limit of detection for the assay. For each virus, groups were compared with an ordinary one-way ANOVA, followed by a Tukey's multiple comparisons test. Statistical significance is indicated as follows: ** = $p \leq 0.01$, *** = $p \leq 0.001$, **** = $p \leq 0.0001$. **D)** Proportion of individuals with a neutralization titer of 1:40 or higher against group 2 viruses (H3, H4, H7) for each age group (n=30 per group) **E–F)** Serum transfer studies in mice (n=5 per group per virus) were performed with pooled serum from each age group (n=30 per group) with subsequent challenge with viruses containing H3, H4 or H7 HAs. Mice that received immunoglobulin depleted serum served as a control. To measure the level of protection, lungs were extracted on day 3 and day 6 post-challenge and virus titers measured by plaque assay. A bar that represents the geometric mean titer is shown for each group. The gray line indicates the limit of detection for the assay. For each virus, groups were compared to the immunoglobulin depleted group with an ordinary one-way ANOVA, followed by a Dunnet's multiple comparisons test. Statistical significance is indicated as follows: ** = $p \leq 0.01$, *** = $p \leq 0.001$, **** = $p \leq 0.0001$.